Contributions of ecological restoration policies to China's land carbon balance

Chao Yue, Mengyang Xu, Philippe Ciais, Shu Tao, Huizhong Shen, Jinfeng Chang, Wei Li, Lei Deng, Junhao He, Yi Leng, et al.

nature communications

Article

https://doi.org/10.1038/s41467-024-54100-9

Contributions of ecological restoration policies to China's land carbon balance

Received: 24 January 2024

Accepted: 30 October 2024

Published online: 09 November 2024

Check for updates

Chao Yue[1,2,3,15] ✉, Mengyang Xu[1,15], Philippe Ciais[4], Shu Tao[5,6], Huizhong Shen[5], Jinfeng Chang[7], Wei Li[8], Lei Deng[2,3], Junhao He[2,3], Yi Leng[8], Yu Li[1], Jiaming Wang[1], Can Xu[9,10], Han Zhang[11], Pengyi Zhang[1], Liankai Zhang[9,10], Jie Zhao[12], Lei Zhu[8] & Shilong Piao[13,14] ✉

Unleashing the land sector's potential for climate mitigation requires purpose-driven changes in land management. However, contributions of past management changes to the current global and regional carbon cycles remain unclear. Here, we use vegetation modelling to reveal how a portfolio of ecological restoration policies has impacted China's terrestrial carbon balance through developing counterfactual 'no-policy' scenarios. Pursuing conventional policies and assuming no changes in climate or atmospheric carbon dioxide (CO_2) since 1980 would have led China's land sector to be a carbon source of 0.11 Pg C yr^{-1} for 2001–2020, in stark contrast to a sink of 175.9 Tg C yr^{-1} in reality. About 72.7% of this difference can be attributed to land management changes, including afforestation and reforestation (49.0%), reduced wood extraction (21.8%), fire prevention and suppression (1.6%) and grassland grazing exclusion (0.3%). The remaining 27.3% come from changes in atmospheric CO_2 (42.2%) and climate (−14.9%). Our results underscore the potential of active land management in achieving 'carbon-neutrality' in China.

The dynamics of the terrestrial ecosystem carbon balance are driven collectively by environmental changes and direct land management[1–4]. Future environmental changes such as climate change and atmospheric CO_2 increase (or decrease) hinge on the climate policies of all nations. Hence, the resulting land carbon responses are beyond the control of any specific nation. In contrast, options for active changes in land management to increase carbon stock or avoid emissions lie within the reach of each individual nation. Indeed, of the declared or submitted nationally determined contributions (NDCs) to implement the Paris Agreement, 10%–30% of the planned reductions in global emissions will be provided by active changes in land management[5,6].

[1]College of Natural Resources and Environment, Northwest A&F University, Yangling, China. [2]State Key Laboratory of Soil Erosion and Dryland Farming on the Loess Plateau, Northwest A&F University, Yangling, China. [3]Institute of Soil and Water Conservation, Northwest A&F University, Yangling, China. [4]Laboratoire des Sciences du Climat et de l'Environnement, LSCE/IPSL, CEA-CNRS-UVSQ, Université Paris-Saclay, Gif-sur-Yvette, France. [5]Guangdong Provincial Observation and Research Station for Coastal Atmosphere and Climate of the Greater Bay Area, Southern University of Science and Technology, Shenzhen, China. [6]College of Urban and Environmental Sciences, Peking University, Beijing, China. [7]College of Environmental and Resource Sciences, Zhejiang University, Hangzhou, China. [8]Department of Earth System Science, Ministry of Education Key Laboratory for Earth System modeling, Institute for Global Change Studies, Tsinghua University, Beijing, China. [9]Kunming General Survey of Natural Resources Center, China Geological Survey, Kunming, China. [10]Technology Innovation Center for Natural Ecosystem Carbon Sink, Ministry of Natural Resources, Kunming, China. [11]College of Economics and Management, Northwest A&F University, Yangling, China. [12]Shandong Provincial Key Laboratory of Water and Soil Conservation and Environmental Protection, College of Resources and Environment, Linyi University, Linyi, China. [13]Sino-French Institute for Earth System Science, College of Urban and Environmental Sciences, Peking University, Beijing, China. [14]State Key Laboratory of Tibetan Plateau Earth System, Resources and Environment, Institute of Tibetan Plateau Research, Chinese Academy of Sciences, Beijing, China. [15]These authors contributed equally: Chao Yue, Mengyang Xu.
✉e-mail: chaoyue@ms.iswc.ac.cn; slpiao@pku.edu.cn

Successful delivery of land-based mitigation potentials, however, requires purpose-driven changes in land management that clearly deviate from the 'no-policy' scenario[7]. While a lot effort has been devoted to quantifying how land management change can contribute to carbon mitigation in the future[8–10], surprisingly, little is known about the contributions of past management changes to current global and regional carbon budgets. The approach used by the global carbon cycle research community focuses on accurately quantifying carbon budgets and the associated land use effects by comparing contemporary land use with the pre-industrial landscape (used to approximate natural vegetation distribution without any human land use or management)[3,11], but it is incapable of revealing the vital contribution of policy-driven active changes in land management, in contrast to the counterfactual 'no-policy' scenarios. Consequently, how changes in past land management have shaped the present-day global and regional terrestrial ecosystem carbon balance remains elusive.

Attributing for changes in land management versus environmental changes using a counter-factual approach, however, faces several obstacles. Separating areas with changes in land management from those without is challenging at fine spatial scales, making any spatially explicit, empirically-based attribution highly uncertain[2,12]. Dynamic global vegetation models (DGVMs) are suitable tools for this purpose as they incorporate both vegetation ecophysiology and human land management processes. However, until recently, most management activities, including forest management (rotation, demography and wood harvest), grassland grazing and fire management, were ignored in the majority of DGVMs used for large-scale assessments of carbon budgets[3]. For example, out of a total of 16 DGVMs used in the Global Carbon Project (GCP) 2022 global carbon budget assessment, only 2 included forest demography and only 6 grassland grazing[3]. None of these DGVMs included active fire suppression or litter raking[3]. Finally, quantifying the contributions of land management changes in contrast to the counterfactual 'no-policy' scenario requires data on the management practices that would have occurred without policy interventions, which are rarely readily available.

In this work, we overcome these obstacles and address the scientific question of how changes in land management versus environmental changes (climate change and atmospheric CO_2 growth) contribute to the contemporary (2001–2020) terrestrial carbon balance in China. Over past decades, substantial management changes occurred in China due to a cluster of ecological restoration projects aiming to restore environmental quality and strengthen carbon sequestration. Given that these policies, or similar ones, are expected to play a crucial role in the nation's strategy for reaching carbon neutrality by 2060[2,8], it is important to know their contributions in the past. For this purpose, we use a DGVM (ORganizing Carbon and Hydrology In Dynamic EcosystEms, ORCHIDEE), which has recently been modified to incorporate a variety of management processes, including afforestation/deforestation, forest rotation, timber and fuelwood extraction and grassland grazing[13]. Additional developments are made in this study to represent active fire control and forest litter raking. We first determine the key ecological restoration projects and their land use effects, and next develop their corresponding 'no-policy' scenarios. Factorial simulations are then used to quantify contributions from land management changes and environmental changes to the country's contemporary terrestrial carbon balance (see Methods).

Results

Land use effects of ecological restoration policies

Before the implementation of the Reform and Opening Policy in 1978, the degradation of natural ecosystems had reached a historical high in China[14]. In response to a land-system sustainability emergency, the Chinese government launched a series of ecological restoration programmes to restore environmental quality and ecosystem services (Fig. 1a and Supplementary Table 1). The land use effects of these programmes fell into five broad aspects: afforestation and/or reforestation, reduced timber harvest, reduced rural fuelwood extraction, grazing exclusion, and decreasing burned areas by forest fires. The impacts of the ecological restoration policies on each of these five aspects are quantified in the following paragraphs and compared with the outcomes of the 'no-policy' scenarios (Fig. 1).

The Three North Shelter Forest Programme, initiated in 1978, was the first large-scale ecological restoration project leading to steadily growing forest area in China (Fig. 1b). The growth accelerated after 2000 following the implementation of several massive afforestation/reforestation projects, including the river shelter projects, the Grain for Green Project and the sand control project. The total forest area growth reached 0.90 (0.81–0.99) Mkm^2 (1 $Mkm^2 = 10^6 km^2$), an increase of 67.7% (60.9–74.4%), during 1981–2020 (Fig. 1b). However, the Land-Use Harmonization version 2 (LUH2) dataset used as the official forcing for the global carbon budget assessments by GCP and also used in the 6th assessment of Intergovernmental Panel on Climate Change (IPCC), failed to account for the policy-driven forest growth (Fig. 1b). Consequently, according to the GCP carbon budget assessments, the land use effects in China have been quantified as a carbon source[15]. For the 'no-policy' scenario, forest areas were assumed to remain unchanged from 1981 onwards.

Human wood extraction considered in this study consists of timber harvest for industrial and household use and rural fuelwood extraction. (1) Reduced timber harvest. The initiation of the Natural Forest Protection Program in 1998 marked a pivotal shift in forest management policy from maximizing returns from timber and tree products to acknowledging the ecological services provided by forest ecosystems[16]. Timber harvesting from natural forests was effectively banned in most parts of China and was shifted to plantation forests. Our results from integrating Food and Agriculture Organization (FAO) data show that domestic timber production decreased from 1996 and maintained a low level (at 1990 values) until around 2005 (Fig. 1c). This stagnation in domestic wood production occurred despite an increasing demand for wood products in line with economic development. Hence, the growing demand was only met by importing more wood from abroad, driving a surge in net timber imports after 1998, which, by 2020, accounted for about a quarter of national timber demand (Fig. 1c). Given that data on China's net timber import is only available from 1990 and the imported amount before 1998 was relatively low, for the 'no-policy' scenario, we make the rough approximation that all timber demand since 1990 would have been met by domestic production (Fig. 1c). (2) Reduced fuelwood extraction. Similar effects of ecological restoration policies on timber production also occurred for fuelwood extraction in rural areas. Driven by both population growth and rural-urban migration, the rural population in China reached a peak around 1990 (Fig. 1d). Accordingly, rural fuelwood extraction increased from less than 150 Tg C yr^{-1} in 1961 to a maximum value in excess of 200 Tg C yr^{-1} around 1990[17]. Its subsequent decline from this peak has been much faster than the decline in rural population (Fig. 1d), as the dominant fuels in the rural energy mix changed from biomass sources (fuelwood, brushwood, straw, etc.) to electricity, biogas, and liquefied petroleum gas[17]. This energy mix transformation was made possible in part by active forest protection policies such as mountain closure and the logging ban, which limited wood accessibility to local farmers. The 'no-policy' scenario used varying rural populations during 1993–2020 but assumed that the value of per capita fuelwood extraction remained constant at the 1992 value (the earliest year for which ground survey data was available, see Tao et al. [17]), and yielded a counterfactual fuelwood consumption of 154.4 Tg C yr^{-1} in 2020, in contrast to 40.9 Tg C yr^{-1} in the real world (Fig. 1d).

Since 2003, China has implemented a policy of returning grazing land to natural grassland (the 'Returning Grazing Land to Grassland Project'). By 2020, the area on which grazing is banned had reached

https://doi.org/10.1038/s41467-024-54100-9

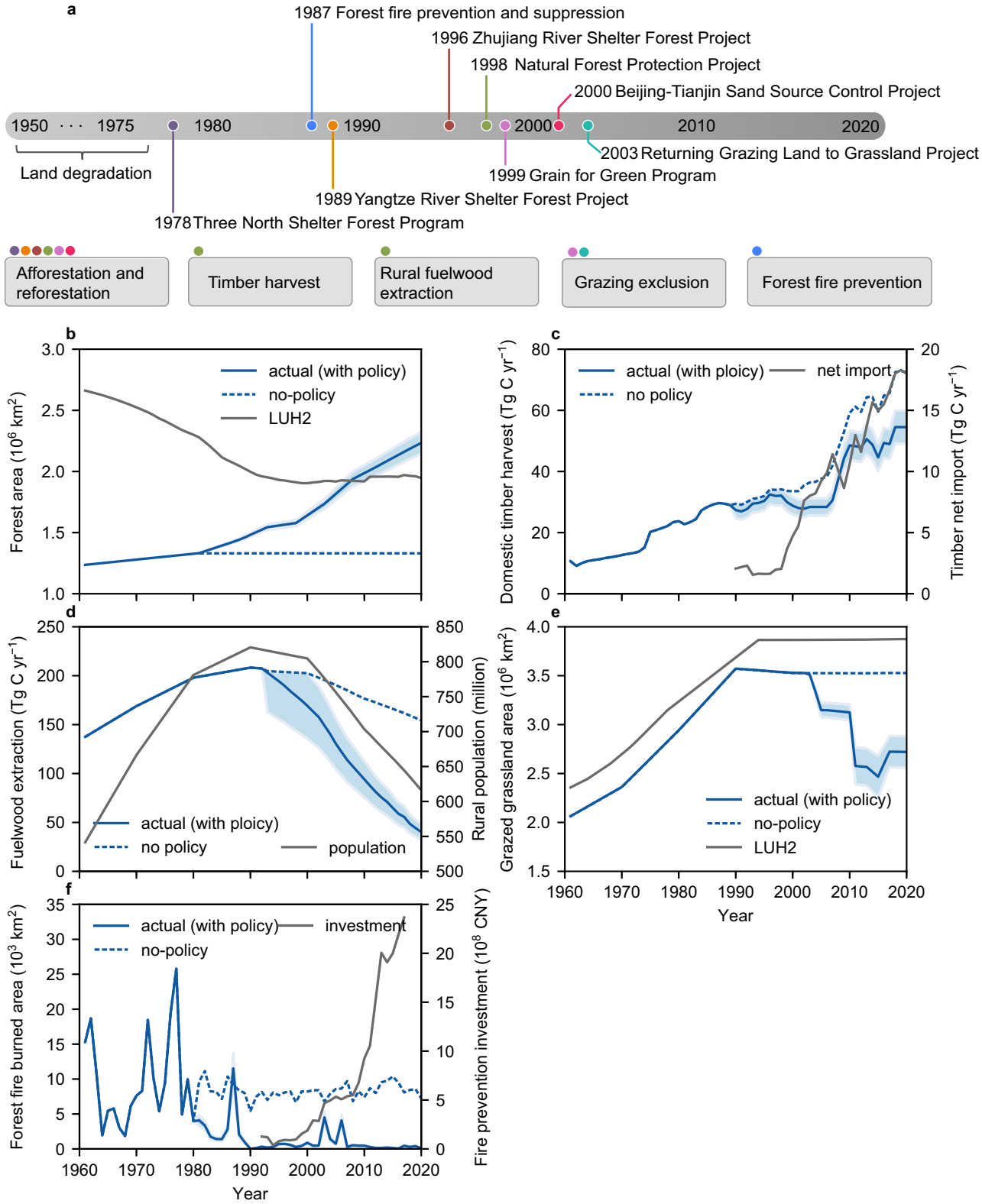

Fig. 1 | Land use effects of ecological restoration policies in contrast to the 'no-policy' scenarios in China during 1981–2020. a Land use effects of the eight key ecological restoration projects implemented in China since the late 1970s were summarized into five aspects (shown as rectangles). Timber harvest and rural fuelwood extraction were further combined as wood extraction. Solid dots in different colours above each rectangle indicate the contributing project(s) (for details refer to Supplementary Table 1). **b**–**f** Actual changes in land use (solid blue lines) with ecological restoration policies in contrast to the counterfactual 'no-policy' scenarios (dashed blue lines). The land use effects of ecological restoration policies were characterized by five different aspects: afforestation and reforestation (**b**), timber harvest (**c**), rural fuelwood extraction (**d**), grazing exclusion (**e**) and forest fire prevention and suppression (**f**). The shading indicates uncertainty (standard deviation). Solid grey lines in (**b**, **e**) show the areas of forest or grazed grassland according to LUH2. The solid grey line in (**c**) shows the net timber import by China (righthand vertical axis). The solid grey line in (**d**) shows the rural population (righthand vertical axis). The solid grey line in (**f**) shows the investment for fire prevention and suppression (righthand vertical axis).

https://doi.org/10.1038/s41467-024-54100-9

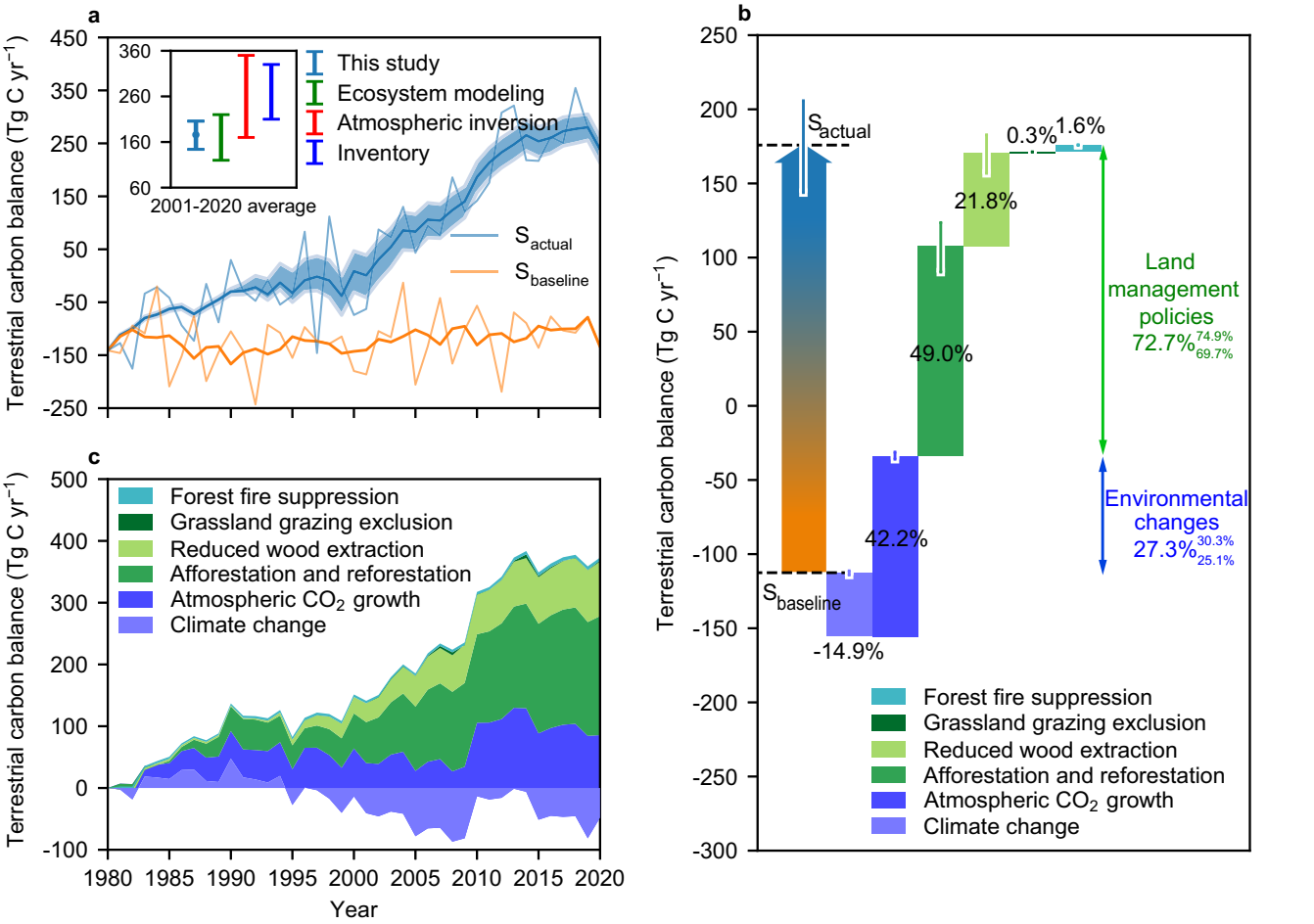

Fig. 2 | Simulated carbon balance over terrestrial ecosystems in China and its driving factors. a Simulated carbon balances under actual conditions (S_{actual}, blue lines) incorporating land management changes due to ecological restoration policies and actual changes in climate and atmospheric CO_2, in contrast to a counterfactual scenario ($S_{baseline}$, orange lines) with 'no-policy' land management practices, cycling climate of 1961–1980 and constant atmospheric CO_2 (1980 value). The thin lines show annual values; the thick lines show 5-year moving averages; the shading shows the standard deviation. Ranges of estimates for 2001–2020 average terrestrial ecosystem carbon sink from independent studies using atmospheric inversion, inventory method, and ecosystem models were obtained from a synthesis study[18] and compared with the value derived in this study in the inset plot. **b** The shift from a counterfactual source for 2001–2020 given by $S_{baseline}$ to an actual sink produced by S_{actual} (represented by the arrow) was attributed to changes in land management and environmental changes. Vertical lines on the bar plots show standard deviations. **c** Temporal patterns of the contributions of different driving factors stacked on top of each other (with individual contributions separately shown in Supplementary Fig. 5). A 5-year moving average was applied for all factors. Reduced wood extraction includes both timber harvest and fuelwood extraction.

0.82 Mkm^2, nearly a quarter of the national grazed grassland (Fig. 1e). Such a decrease in grazed grassland has not been accounted for in the LUH2 dataset which was based on, but is slightly different from, the History database of the Global Environment (HYDE3.2). The 'no-policy' scenario hence used the grazing areas reported by HYDE3.2 (by summing the 'pasture' and 'rangeland' values) which did not account for the grazing exclusion policy in China (Fig. 1e).

China has systematically strengthened its institutional capacities for forest fire prevention and suppression following an iconic catastrophic forest fire in 1987. The investment in forest fire prevention and suppression has increased by more than 15 times between 1993 and 2017 (Fig. 1f). Accordingly, the mean annual area burned by forest fires during 2001–2020 (0.78×10^3 km^2) was reduced by more than by 90% compared to 1987 (11.5×10^3 km^2). For the 'no-policy' scenario, simulated burned areas for forests in China obtained from prognostic fire modules embedded within five DGVMs were used (see Methods). These models do not account for the fire prevention and suppression policy in China, resulting in forest fire dynamics primarily driven by climate variations (Fig. 1f). The counterfactual area burned by forest fires under the 'no-policy' scenario was 8.48×10^3 km^2 yr^{-1} for 2001–2020, about ten times greater than the actual area.

Management and environmental contributions to land carbon balance

The ORCHIDEE model incorporating land management changes due to ecological restoration policies and time-varying climate and atmospheric CO_2 changes (S_{actual}) simulated a carbon sink of 175.9 (143.8–205.8) Tg C yr^{-1} in China's terrestrial ecosystems during 2001–2020 (Fig. 2a). The sinks were mainly located in forest ecosystems, and were dominated by increases in biomass with only a small contribution from soil carbon (Supplementary Table 2). This simulated sink lies within the range of 120–350 Tg C yr^{-1} derived by different approaches including forest inventory, atmospheric inversion, and other DGVMs[15,18–20] (Fig. 2a). Alternatively, the 'no-policy' land management scenario combined with cycling the climate conditions of 1961–1980 while maintaining atmospheric CO_2 at its 1980 value ($S_{baseline}$) yielded a carbon source of −112.5 Tg C yr^{-1} over the same period. The difference of 288.4 (256.3–318.3) Tg C yr^{-1} between S_{actual} and $S_{baseline}$ for 2001–2020 was thus attributed to the changes in land

management and in environmental conditions (the thick arrow in Fig. 2b).

Our attribution analysis showed that 72.7% (69.7–74.9%, or 178.6–238.5 Tg C yr^{-1}) of the difference could be attributed to changes in land management, of which 49.0% (48.4–49.5%, or 124.1–157.5 Tg C yr^{-1}) was contributed by afforestation and reforestation, 21.8% (19.2–23.6%, or 49.3–75.3 Tg C yr^{-1}) by reduced wood extraction, 0.3% (0.3–0.3%, or 0.9–0.9 Tg C yr^{-1}) by grazing exclusion and 1.6% (1.5–1.7%, or 4.4–4.9 Tg C yr^{-1}) by forest fire prevention and suppression (Fig. 2b). Changes in environmental conditions contributed 27.3% (25.1–30.3%, or 77.8–79.8 Tg C yr^{-1}) of the difference, consisting of a positive contribution of 42.2% (39.0–46.6%, or 119.4–124.3 Tg C yr^{-1}) from the atmospheric CO_2 increase, being partly offset by a negative one of −14.9% (−16.2 to −14.0%, or −44.5 to −41.6 Tg C yr^{-1}) from climate change (Fig. 2b). The contribution of each individual factor reported here includes both the direct effect and the interactive effect with other factors (see Methods). Our analysis, by performing additional simulations to separate the direct effect, shows that the direct effects accounted for 88.5% of the total effects (79.5% for environmental changes and 91.8% for land management changes), with the interactive effects among different factors accounting for 11.5% (Supplementary Table 3).

Afforestation and reforestation were found to have increased forest areas of all ages (Supplementary Fig. 1), whereas reductions in wood extraction and forest fires mainly allowed old-aged secondary forests to recover (Supplementary Figs. 2 and 3). These, along with an increase in biomass with forest growth (Supplementary Fig. 4), explained the increase in simulated forest carbon balance from a negligible source of −7.0 Tg C yr^{-1} in the 1980s to a strong sink of 259.3 Tg C yr^{-1} in the 2010s (Supplementary Table 4). This result is supported by national forest inventories (NFIs) and large-scale ground surveys, which have reported that the forest carbon sink in China increased from 17.0 Tg C yr^{-1} in the 1970s–80s to 75.0 Tg C yr^{-1} in the 1990s–2000s and further to 160.0 Tg C yr^{-1} during 2001–2010[21,22] (Supplementary Table 5).

Changes in climate over 1981–2020, compared with the cycling climate of 1961–1980, showed a positive contribution to China's terrestrial carbon sink during the initial two decades, followed by a shift to a negative contribution during the latter two decades (Fig. 2c). Such temporal variations of the climate contribution seem to be mainly driven by changes in precipitation and surface air humidity, as annual surface air temperature during 1981–2020 was largely higher than its value in 1961–1980 (Supplementary Fig. 6). The ORCHIDEE simulation showed a significant ($p < 0.05$) positive correlation between the change in China's terrestrial carbon balance (net biome production, ΔNBP) and the change in annual precipitation (ΔP), as well as a positive, albeit non-significant ($p = 0.16$), correlation between ΔNBP and the change in surface air humidity, but a significant ($p < 0.01$) negative correlation between ΔNBP and the change in annual surface air temperature (ΔT) was found (Supplementary Fig. 7).

The positive correlation between ΔNBP and ΔP and the negative one between ΔNBP and ΔT has been previously reported by Zhang et al. [19] who used six ecosystem models over China. In particular, the negative correlation between ΔNBP and ΔT reported by Zhang et al. [19] was found to be due to a greater stimulation by temperature increase of ecosystem respiration than of ecosystem productivity[19]. A similar effect was found in this study (northeastern China in Supplementary Fig. 8) and has been confirmed by global multi-model simulations over temperate regions[23]. In addition, previous analysis of satellite-based vegetation greenness (a proxy for productivity) and surface temperature reveals their correlation to be positive only for northern boreal regions and negative for temperate regions[24]: a result consistent with the modelling evidence for China[19,23] which is dominated by temperate climate.

Compared to the cycling climate of 1961–1980, the first half of 1981–2020 was marked by a moderate warming but there was also a clear increase in surface air humidity, accompanied by a moderate increase in precipitation (Supplementary Fig. 6). It is likely that the positive effects of increasing precipitation and air humidity outweigh the negative effect of increasing temperature, explaining the small positive contribution of climate change to China's terrestrial carbon sink. For 2001–2020, pronounced warming and decreases in both precipitation and surface air humidity explain the negative contribution of climate change. In contrast, the contributions of atmospheric CO_2 growth, afforestation/reforestation, and reduced wood extraction showed continual increases with time, whereas the contributions from grassland grazing exclusion and forest fire suppression remained small throughout the study period (Fig. 2c).

Spatial patterns of management and environmental contributions

Spatially, S_{actual} revealed an extensive carbon sink mainly dominated by forest ecosystems (Fig. 3a and Supplementary Fig. 9a). There were sporadic carbon sources in northeastern China, mainly in cropland areas (Supplementary Fig. 9b), while in Tibet and Sichuan provinces, the carbon sources were in grazed grassland (Supplementary Fig. 9d, see Supplementary Fig. 10 for a map with provincial names). In contrast, $S_{baseline}$ showed pervasive carbon sources across almost the entire country (Fig. 3b). Hence, the difference between the S_{actual} and $S_{baseline}$ simulations, i.e. contributions from changes in land management and environmental conditions, showed a widespread carbon sink effect (Fig. 3c).

The changes in climate conditions during 2001–2020 in contrast to 1961–1980 mainly exerted a carbon source effect (Figs. 2c and 3d), with a spatial pattern largely corresponding to those of changes in precipitation and surface air humidity, rather than changes in temperature (Supplementary Fig. 11). For many parts of the country, annual precipitation decreased, especially over southwestern China (Yunnan and Guizhou provinces) and the region circling the Bohai Sea (Supplementary Fig. 11). Although precipitation increased in southeastern China, the surface air humidity showed a decline, likely because of increasing atmospheric water demand associated with the temperature increase (Supplementary Fig. 11). For northwestern China, Xinjiang province and the Qinghai–Tibet Plateau, both precipitation and surface air humidity increased, despite the temperature increase (Supplementary Fig. 11).

The decreases in precipitation in southwestern and northern China caused remarkable reductions in gross photosynthetic uptake (Supplementary Fig. 8a), explaining the negative effect of climate change on the terrestrial carbon sink in these regions (Fig. 3d). Although higher precipitation combined with warming did increase ecosystem productivity in northeastern and southeastern China (Supplementary Fig. 8a), such increases were largely offset by growing ecosystem respiration (Supplementary Fig. 8b), resulting in a reduced terrestrial carbon sink (Supplementary Fig. 8c, Fig. 3d). This result is consistent with the results of the multi-model global simulations[23], which show that anthropogenic climate warming has generally reduced the terrestrial carbon sink over tropical and temperate regions across the globe (including China). In contrast, in Xinjiang and Qinghai–Tibet Plateau, where vegetation growth is largely temperature-limited[24,25], warming and wetting mostly increased the terrestrial carbon sink (Supplementary Fig. 8c, Fig. 3d).

Both Xu et al. [26] and Zhang et al. [27] have reported long-term declines in water availability in China over 1981–2010. Drought events have been individually documented in southwestern China (Yunnan and Guizhou) during 2009–2010[28] and in southern China in 2013[29]. These events are reported to have reduced vegetation greenness and the associated gross primary production (GPP)[28,29]. The reported decline in China's terrestrial carbon sink in 2001–2020 compared to 1961–1980, mostly driven by decreased water availability, is, hence, consistent with these observations. The atmospheric CO_2 increase

https://doi.org/10.1038/s41467-024-54100-9

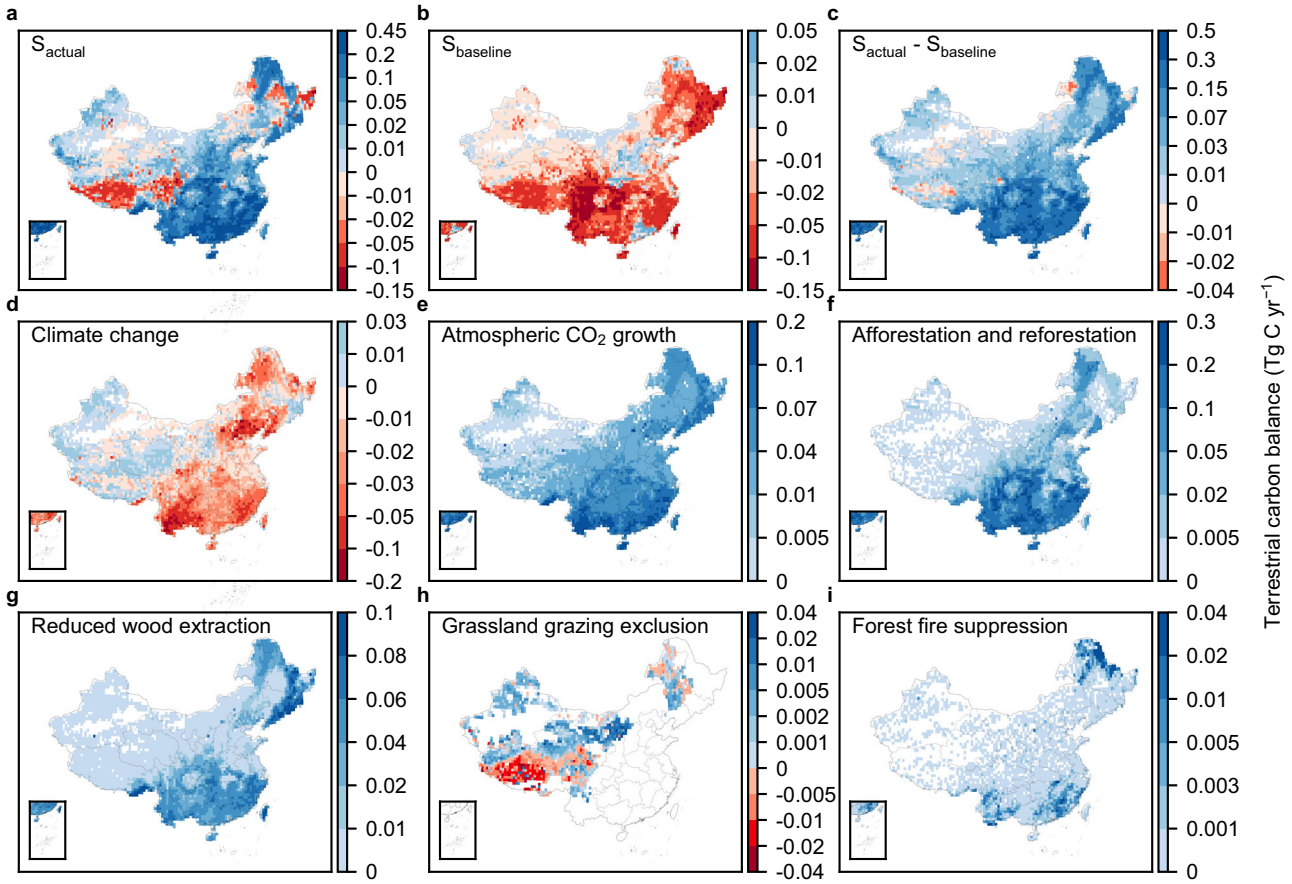

Fig. 3 | Spatial patterns of simulated terrestrial carbon balances and contributions from different driving factors for 2001–2020. Spatial patterns of simulated land carbon balances by S_{actual} (**a**), $S_{baseline}$ (**b**) and the collective contributions of changes in land management and environmental conditions, i.e. the difference between S_{actual} and $S_{baseline}$ (**c**). Spatial patterns of contributions by each individual factor of climate change (**d**), atmospheric CO_2 growth (**e**), afforestation and reforestation (**f**), reduced wood extraction, including both timber harvest and fuelwood extraction (**g**), grassland grazing exclusion (**h**) and active forest fire suppression (**i**). See Supplementary Fig. 10 for the names of different provinces in China.

during 2001–2020 compared to its 1980 level, however, led to a widespread positive contribution (Fig. 3e).

Among all the land management factors considered, spatially, afforestation and reforestation show the greatest contribution to the terrestrial carbon sink in 2001–2020 (Figs. 2b and 3f). Its spatial pattern corresponds well with that of forest expansion, with large increases found along the transect from northeastern to southwestern China (i.e. eastern and southern Inner Mongolia, the provinces of Shaanxi, Sichuan, Guizhou and Yunnan), southern China (Guangxi Province) and southeastern China (the provinces of Jiangxi, Zhejiang and Fujian) (Supplementary Fig. 12a). The contributions of reduced wood extraction have a similar spatial distribution to the reductions in timber harvest and fuelwood extraction (Fig. 3g and Supplementary Fig. 12b–d). Da Xing'an, Xiao Xing'an and Changbai Mountains in northeastern China have notable increases in carbon sink, mainly due to reductions in timber harvest (Supplementary Fig. 12c), whereas increases in the carbon sink in vast areas of southwestern, southern and southeastern China can be attributed to reductions in fuelwood extraction (Supplementary Fig. 12d).

A recent synthesis of China's grassland carbon balance revealed great uncertainties in its estimation[30], with values ranging from a source of −3.4 Tg C yr^{-1} to a mild sink of 15 Tg C yr^{-1}. ORCHIDEE simulated the carbon balance of natural grassland in China as ranging from −14.3 to 16.3 Tg C yr^{-1}, while that of grazed grassland was a mild source of −3.0 to −34.3 Tg C yr^{-1} (Supplementary Table 4). Grazing exclusion, however, generally made a small contribution to the land carbon sink, with a positive contribution of 4.0 Tg C yr^{-1} being offset by a negative one of −3.1 Tg C yr^{-1} (Fig. 3h). Northern and northwestern China, where vast areas of grassland were subject to grazing exclusion (Supplementary Fig. 12e), showed considerable carbon sink effects, whereas in southwestern (Yunnan and Sichuan) and southern China (Guangxi and Guangdong), where the grazing exclusion areas were relatively small, the contributions were mild (Supplementary Fig. 12e). The areas showing a negative contribution from grazing exclusion, including northeastern China and Tibet, mainly have low grazing stock densities (Supplementary Fig. 13), a pattern which is consistent with field observations showing that light grazing can increase terrestrial carbon stock in China[31].

The 90% reductions in burned area in forest ecosystems have resulted in, on average, a 4.6 Tg C yr^{-1} larger carbon sink for 2001–2020, with direct fire emissions being reduced by 3.3 Tg C yr^{-1} and an increase in forest NBP of 1.3 Tg C yr^{-1}. Reductions in burned area and the corresponding increases in the carbon sink were mainly found in mountainous regions in northeastern, southwestern, and southeastern China, where fire prevention and suppression have greatly reduced forest fires (Fig. 3i and Supplementary Fig. 12f).

The land use and land management datasets were well constrained on prefectural (rural fuelwood extraction), provincial (afforestation and reforestation, cropland area) and national (timber harvest, grazing exclusion, and forest fire burned area) scales (see Methods). The spatial allocation of prefectural, provincial or national total values of land use and land management to grid cells either follows satellite observations and state-of-the-art land use products, or, when no such observation-based datasets are available, is based on

reasonable assumptions (Supplementary Method 1, Supplementary Table 6). Often, there are no alternative more reliable datasets which would allow quantification of spatial allocation errors and uncertainties (with the exception of cropland, see Supplementary Discussion 1). Hence, a qualitative assessment of the uncertainty in the spatial pattern of land use and land management is provided as Supplementary Table 6. Small uncertainties were assigned to the spatial pattern of the carbon sink contributions of afforestation/reforestation and forest fire suppression. For the contribution of reduced wood extraction, a small uncertainty was assigned to rural fuelwood extraction, which dominates the total reduction in wood extraction due to ecological restoration (Fig. 1c, d), while a large uncertainty was assigned to timber production. A medium level of uncertainty was assigned to the contribution of grazing exclusion.

The impacts on the simulated terrestrial NBP by the S_{actual} simulation over 2001–2020 and its spatial distribution resulting from the uncertainties in cropland spatial distribution were additionally investigated through adjusting the cropland distribution in this study to match that provided by a reconstruction of China's cropland distribution over 1900–2016. This reconstruction integrated datasets from multiple sources and is considered to be more reliable over China than HYDE3.2 (Supplementary Discussion 1). The results show that, for 90% of grid cells, the uncertainties in the simulated NBP over 2001–2016 were less than 0.01 Tg C yr^{-1}—a relatively small value (Supplementary Fig. 14). The national NBP, on average, 2.2 Tg C yr^{-1} lower after the adjustment for 2001–2016, well within the uncertainty range of (−33.2, +31.1) Tg C yr^{-1} of the initially estimated value (Fig. 2a, Supplementary Fig. 14). These results illustrate a small impact of the uncertainty in the spatial distribution of cropland on the simulated national NBP. Furthermore, as the influences of cropland distribution will be filtered out when comparing simulated NBP between S_{actual} and $S_{baseline}$, the contributions of different land management changes shown in Fig. 3 are expected to be little impacted by any uncertainty in cropland distribution.

In terms of regional distributions, the three regions of southern China (Southwest, South, and Southeast) account for more than 60% of the national total effect (Fig. 4), with the biggest contribution coming from the Southwest (89.9 (81.0–98.6) Tg C yr^{-1}), followed by Southeast (51.8 (45.7–51.8) Tg C yr^{-1}) and South (37.2 (34.1–40.2) Tg C yr^{-1}). Contributions from the three regions in northern China were comparable to each other, ranging from 24.8 (23.2–26.8) Tg C yr^{-1} in North and 32.7 (27.9–38.6) Tg C yr^{-1} in Northeast (Fig. 4). In northern China (Northwest, North, and Northeast), increases in atmospheric CO_2 concentration made the biggest contribution, whereas in southern China, afforestation and reforestation was the most important factor. Northwest is the only region where the contribution of environmental changes outweighed that of land management policy and where climate change made a positive contribution (4.5 (4.4–4.7) Tg C yr^{-1}) (Fig. 4b), as a result of improved water availability. In Northeast, forest fire suppression made a notable contribution of 6.1% (5.4–7.1%) to the enhanced carbon sink, mainly because of prominent reductions in burned areas (Supplementary Fig. 12f).

Uncertainties and implications

The uncertainty of our results resides mainly in the formulation of the 'no-policy' management scenarios and the choice of reference climate and atmospheric CO_2 used in the $S_{baseline}$ simulation. Based on our research period of 1981–2020, the atmospheric CO_2 concentration for $S_{baseline}$ was chosen as being fixed at its value in the starting year of 1980. We further assumed that the atmospheric general circulation patterns, without changes being driven by atmospheric CO_2 growth since 1980, would have resembled those during the preceding 20 years, explaining our choice to use the climate conditions of 1961–1980 as the reference climate.

Previous studies have shown that nitrogen deposition contributes about 10–20% to the terrestrial carbon sink in China[15,20]. Because nitrogen cycling was not represented in the ORCHIDEE version used in this study, nitrogen deposition was not explicitly addressed here, which might lead to an underestimation of the environmental contribution. However, the effects of nitrogen deposition on carbon sequestration were (partly) implicitly accounted for in the CO_2 effects because model parameters were tuned to ensure that simulated forest biomass growth and vegetation productivity largely matched the observations, which were subject to the influences of nitrogen deposition (Supplementary Table 7, Supplementary Figs. 4 and 15). In this study, vegetation net primary production (NPP) and biomass carbon stock were simulated to increase by 12.7% and 15.8%, respectively, for an increase in atmospheric CO_2 concentration of 100 ppm. These sensitivity values fall within or are at the high end of, the range of atmospheric CO_2 sensitivities obtained by a recent synthesis of CO_2 enrichment experiments[32]: According to ref. 32, for NPP, the observed 95th quantile interval is [1.4%, 14.2%] with a mean value of 7.8%; for biomass stock, the observed 95th quantile interval is [8.1%, 15.2%] with a mean value of 11.7%. The fact that nitrogen deposition was partly accounted for in the CO_2 fertilization effect through parameter tuning might help to explain the comparatively high CO_2 sensitivity simulated by ORCHIDEE, potentially leading to an overestimated CO_2 fertilization effect on China's terrestrial carbon sink.

Clearly, such parameter tuning to implicitly account for nitrogen deposition is suboptimal. Nitrogen deposition in China increased from 1980 onwards but began to stabilize after 2005[33]. There has been a decline since 2010[34], and further decrease has been projected for the future, as the implementation of clean air and 'carbon neutrality' policies is expected to reduce both carbon emissions and the associated air pollution[35]. As a result, future carbon sinks may reduce in response to decreasing nitrogen deposition[36]. Nitrogen cycling has already been integrated in another version of ORCHIDEE but future model developments need to integrate the functionalities of both land management and nitrogen cycling in a single version of ORCHIDEE, to allow for mechanistic simulations of carbon cycle impacts of both the dynamics of land management and nitrogen deposition.

Note that the quantified contributions from changes in land management, however, were little influenced by the chosen reference environmental conditions, because actual environmental changes were used in both the S_{actual} simulation and the respective baseline simulations with 'no-policy' land management (Supplementary Tables 8–10). Hence, the obtained contributions from land management policies are robust, given the 'no-policy' scenarios developed in this study. Our approach to quantifying the contribution of each individual land management process, i.e. by pairing two cases with and without ecological restoration policy while using realistic environmental conditions, was conceptually similar to that of a previous study by Lu et al. [2], where carbon sequestration rates for a pair of adjacent sites with and without ecological restoration were compared to derive the policy effect[2]. With almost the same scope of ecological restoration projects as in this study, except for forest fire control, Lu et al. [2] used a systematic ground survey to conclude that ecological restoration policies contributed to 56% of the land carbon sink in China, a proportion close to our estimate. Neither Lu et al. [2] nor our study included the effects of crop management changes (residual management and fertilization) or soil erosion control policies, which, according to independent empirical estimates, contribute about 10% and 8%, respectively, to the terrestrial carbon sink in China but are subject to great uncertainties[37,38].

The ORCHIDEE model used here incorporates multiple functionalities of forest demography, afforestation/reforestation, wood harvest followed by forest regeneration, grassland grazing, litter raking, and forest fire suppression (with the latter two functionalities additionally developed in this study), making it suitable for investigating

https://doi.org/10.1038/s41467-024-54100-9

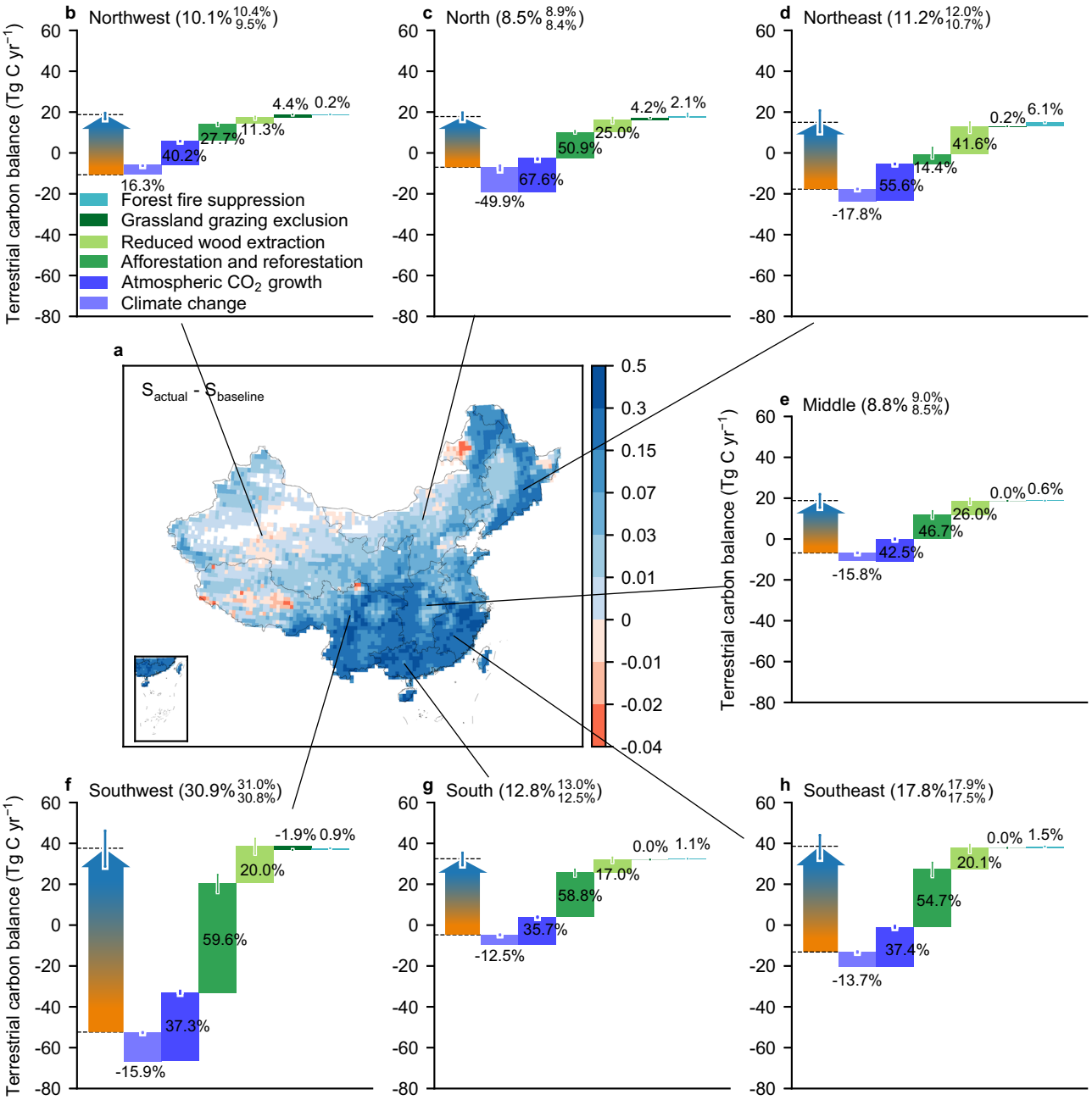

Fig. 4 | Contributions of changes in land management and environmental conditions to the terrestrial carbon balance in the seven regions over 2001–2020. The central map (**a**) displays the difference in simulated land carbon balance between S_{actual} and $S_{baseline}$ (repeating Fig. 3c). shows the shift from the counterfactual carbon source given by $S_{baseline}$ to an actual sink by S_{actual} (indicated by the arrows) and the contribution from each individual driving factor for Northwest (**b**), North (**c**), Northeast (**d**), Middle (**e**), Southwest (**f**), South (**g**), and Southeast (**h**). Vertical lines on the bar plot show the uncertainty (standard deviation). Reduced wood extraction includes both timber harvest and fuelwood extraction.

the relative contributions of various land management types to China's terrestrial carbon balance. Our results reveal that active changes in land management have dominated increases in the terrestrial carbon sink over the past four decades in China. In particular, these contributions have been dominated by changes in the forest sector, including increases in forest area, reduced wood extraction, and forest fire control. This is consistent with recent findings that highlighted the dominant mitigation potential of forests in future natural climate solutions in China, with relatively small contributions from grassland, cropland, and wetland[8].

Recently, the role of secondary forests in global and regional forest carbon sinks has gained increasing attention[39], emphasising the need for DGVMs to incorporate forest demography[40]. Our results show that afforestation and reforestation increase forest areas of all age classes in China but the most prominent increases were found in the young and middle-aged classes (Age 2 to Age 5, Supplementary Fig. 1), while the area increase in the oldest age class (Age 6) was mainly driven by forest aging. Two very recent studies based on DGVM simulations with forest demography in China[41,42], with ref. 41 using the same ORCHIDEE version as in this study, showed that forest aging combined with forest area expansion is an important driver of the contemporary forest carbon sink in China, but forest aging alone will lead to a decline of 30%–40% in the forest carbon sink by the end of this century. These results highlight the need to explicitly incorporate forest demography

in accurately predicting forest carbon dynamics. They also highlight that, for a forest carbon sink of its current size to be sustained in China, additional afforestation and reforestation will be needed.

In contrast to forest expansion, the contributions of changes in wood extraction to China's forest carbon sink have been much less investigated. One of the limiting factors here is a lack of reliable rural fuelwood extraction data. Based on our peer-reviewed dataset derived from systematic ground surveys spanning 346 prefectures in China, we reported a reduction of 168.1 Tg C yr^{-1} in rural fuelwood extraction in 2020 compared to its peak value around 1990. Considering timber harvest further, ecological restoration policies were found to have reduced wood extraction by, on average, 93.6 Tg C yr^{-1} during 2001–2020 (81.4 Tg C yr^{-1} from fuelwood extraction and 12.2 Tg C yr^{-1} from timber harvest), resulting in a forest sink of 62.8 (49.3–75.3) Tg C yr^{-1}. Through the hypothetical suppression of a timber harvest of 55 Tg C yr^{-1}, Yu et al. [42] used a DGVM to simulate a forest biomass carbon increase of about 42 Tg C yr^{-1} over 2020–2050, which, if adjusted proportionally according to the reduction in wood extraction in this study, would translate into a forest biomass carbon sink of 71 Tg C yr^{-1}. This value is slightly higher than our estimate but still falls within our uncertainty range. In addition, the carbon sink effects of reduced rural fuelwood extraction are also supported by a recent study[43], which combined rural-urban population migration and satellite-derived forest biomass change to show that rural depopulation has resulted in an increase in forest biomass carbon stock in southern China.

The dedicated model development of forest fire impacts on forest age dynamics in this study puts us in the unique position of being able to investigate the effect of forest fire suppression on China's forest carbon balance. Our analysis shows that forest fire suppression in China has reduced burned area from an estimated 8.48×10^3 $km^2 yr^{-1}$ under the 'no-policy' scenario to 0.78×10^3 $km^2 yr^{-1}$ in reality—a 90% reduction over 2001–2020. A human-induced reduction in wildfire areas with a similar relative percentage has occurred in the USA: national wildfire area has decreased from 230×10^3 km^2 in the 1930s to about 30×10^3 km^2 ha in the 2000s, with a relative decrease of 87%, largely due to fire suppression and fire exclusion[44]. Reduction in wildfire was found to dominate the land management-associated terrestrial carbon sink in North America for 1950–2000[45]. Given that forest carbon sinks over 2001–2020 were similar for China and the USA[46] but the reduction in burned area in China was two orders of magnitude smaller than in the USA, the contribution of China's forest fire suppression to its terrestrial carbon sink growth was also quite small on the national scale (1.6% (1.5%–1.7%), or 4.6 (4.4–4.9) Tg C yr^{-1} over 2001–2020) but was regionally important (e.g. the Northeast).

Both reduced wood extraction and forest fire suppression were found to have stimulated old forest recovery (Supplementary Figs. 2 and 3). As carbon stocks in old-growth forests will ultimately become saturated[47] if there are no further reductions in wood extraction and fire suppression in the future, the carbon benefits from these land management will become limited.

Future carbon sequestration of land ecosystems depends on both environmental changes and land management and their interplay. As many nations have announced targets of net zero emissions in response to the urgent need to halt global warming, limited contributions of environmental changes to terrestrial carbon sequestration can be expected in the future. Hence, active land management will turn out to be crucial in enhancing land carbon uptake. However, as secondary forests arising from afforestation/reforestation, wood extraction reduction and fire suppression enter their old-growth state, their carbon uptake will inevitably decline[41,42]. Sustaining a substantial amount of land carbon sequestration hence demands further forest expansion, possibly with careful species selection to further boost carbon storage[48], as well as improved forest management practices such as tending, rotation length extension and an extended lifetime for wood products[42]. On the other hand, future climate change might increase the frequency of forest disturbances such as drought, fire and insect outbreaks[49] and hence threaten the stability of forest carbon stock. Therefore, proactive management is needed to address these upcoming challenges while aiming to enhance both the size and stability of forest carbon stock. Future model developments hence need to further improve the representation of forest management and various disturbances beyond forest fire considered in this study. In addition, the functions of cropland management including residual management and fertilization, and lateral carbon transfer including soil erosion and sediment transport[50], should also be integrated to enable an holistic evaluation of future land carbon sink potential under changing climate conditions.

Methods

Model description

ORCHIDEE is a process-based DGVM designed to simulate carbon, water and energy fluxes in various vegetation ecosystems, operating from site level to the global scale[51–53]. As in most DGVMs, vegetation types are discretized into plant functional types (PFTs) (a total of 15 PFTs, Supplementary Table 7). The ORCHIDEE version used in this study was ORCHIDEE-MICT-GLUC (ORganising Carbon and Hydrology in Dynamic EcosystEms-aMeliorated Interactions between Carbon and Temperature-Gross Land-Use Change), recently developed to account for various land use processes, including deforestation/afforestation, forest management (wood harvest and forest rotation), shifting cultivation, fire disturbance, and grassland grazing[54]. Grazed grasslands were distinguished from natural grasslands by assuming domestic grazing over the former but no grazing over the latter. Additionally, this version accounts for forest age structure at subgrid scales and hence allows the characterization of forest age dynamics in response to land management changes (Supplementary Figs. 1–3 and 16). Forest age was expressed as age classes rather than specific years since forest establishment or regeneration. There are six age classes for each forest PFT, from young to old, denoted as Age 1 to Age 6 (Supplementary Figs. 1–3 and 16). For details on forest age class representation, please refer to Supplementary Method 2. In addition, the model's representation of fire-induced forest mortality and litter raking processes were further developed to cater for our research purposes.

Additional model developments

(1) Accounting for the effects of fire-driven mortality on forest age dynamics. China has been imposing strict forest fire prevention and suppression policies since the late 1980s. As a result, nationally, the area burned by forest fires has drastically decreased. Fires which do successfully escape initial suppression are often a result of extreme fire weather and lead to stand-replacing mortality followed by forest regeneration[55]. Fire-induced tree mortality at the stand scale was originally simulated in ORCHIDEE using a dilution approach, in which the regenerating forest stand was merged with existing forests, with all carbon pools and carbon fluxes being aggregated. However, this approach failed to faithfully represent the stand-replacing effect of fires on forest age dynamics. Hence, the model was modified to represent the stand-replacing effect of forest fires, so that a young forest cohort was explicitly established at a sub-grid scale and independently tracked. With this improved approach, old-growth forests were simulated to recover from declining fire activity (Supplementary Fig. 3). Fire-driven mortality rates for different forest PFTs were prescribed using satellite-derived mortality rates (see Supplementary Method 3 and Supplementary Table 7). (2) Litter raking by rural fuelwood consumption. Part of the fuelwood extraction in rural areas in China is not through intentional forest cutting but from forest litter raking. This process was additionally included in ORCHIDEE by simply removing the demanded fuelwood carbon from litter in forest PFTs, taking contributions from different types of aboveground litter

(including both metabolic and structural litter types with different turnover rates) in proportion to their existing mass. Surface fuel availability, which limits fire occurrence, was updated following forest litter raking.

Representing ecological restoration and the 'no-policy' scenarios

This section explains how the land use effects of active changes in land management, in contrast to the effects in the 'no-policy' scenarios, were incorporated in ORCHIDEE. Detailed information on the preparation of spatially explicit forcing data is provided in the Section 'Forcing datasets for different factorial simulations' in Methods.

The land use effects of ecological restoration policies were characterized by five different aspects: afforestation and reforestation, timber harvest, rural fuelwood extraction, grazing exclusion and forest fire prevention and suppression (Fig. 1). Detailed descriptions of the ecological restoration projects and their linkages to these five aspects are presented in Supplementary Table 1. For each aspect, actual changes in land use were determined, with their effects on land carbon cycle processes being simulated by ORCHIDEE. In contrast, counterfactual land use effects under the 'no-policy' scenarios, i.e. without ecological restoration policies, were also developed and simulated (Supplementary Table 8). Differences in simulated terrestrial carbon fluxes between the actual and 'no-policy' scenarios were diagnosed as the carbon cycle effects of active changes in land management. Because large-scale ecological restoration policies were only implemented from the late 1970s or early 1980s onwards, their carbon cycle effects were examined for 1981–2020, with a specific focus on 2001–2020.

Afforestation and reforestation were represented in ORCHIDEE as increases in the forest area at the cost of cropland, natural grassland or grazed grassland. Several ecological restoration projects, including the Three North Shelter Forest Programme, the River Shelter Forest projects and the Grain for Green project, have contributed to nationwide forest area growth. According to the NFIs, the forest area has increased from 1.35 Mkm^2 (1 $Mkm^2 = 10^6$ km^2) for the 2nd NFI (1977–1981) to 2.23 Mkm^2 for the 9th NFI (2014–2018) (Fig. 1b). For the 'no-policy' scenario, forest area was assumed constant after 1981 (Supplementary Table 8).

Timber harvest was represented in ORCHIDEE by forest cutting followed by harvesting aboveground sapwood and heartwood, with belowground biomass and the unharvested aboveground components being transferred to the litter pool. Part of the rural fuelwood extraction was simulated the same way as the industrial timber harvest, with the remaining part simulated in the form of forest litter raking. No data were available to determine the fraction of fuelwood extracted through litter raking, but a value exceeding a range of 30% to 70% was considered unlikely. We hence performed two simulations with the value set at 70% and 30%, respectively. The results indicated a very low sensitivity to the value of this fraction in the quantified contribution of reduced fuelwood extraction to the land carbon sink over 2001–2020 (i.e. 22% when assuming a fraction of 70% and 23% for a fraction of 30%) and, therefore, the value was set as 70%.

Ecological restoration projects, such as the Natural Forest Protection Project implemented in 1998, were believed to have limited or reduced both timber harvest and rural fuelwood extraction (Supplementary Table 1). As a result, domestic timber production fell slightly during 1996–2005, but the share of China's timber demand satisfied through import has surged since 1998 (Fig. 1c). On the other hand, following the peak in rural fuelwood extraction in 1990, decreases have been faster than those driven solely by the decreasing rural population, because, in response to more stringent forest protection policies, a higher share of rural energy demand has been met by electricity, biogas or liquefied petroleum gas rather than fuelwood. Hence the 'no-policy' scenario assumed that all timber demand in China was met by domestic harvest (after 1990) and rural fuelwood extraction (after 1992) followed the predicted fuelwood demand driven only by changes in rural population for 1992–2020 with no changes in the rural energy mix (Fig. 1d and Supplementary Table 8).

In ORCHIDEE, two types of grassland were simulated: grazed grassland or pasture that was grazed by domestic livestock, and natural grasslands on which there was no grazing. Grazing exclusion was represented by a transition from grazed grasslands to natural grassland. The Chinese government launched the 'Returning Grazing Lands to Grasslands Project' in 2003 in order to halt the widespread grassland degradation due to overgrazing. According to China's Land Greening Bulletin 2020 (https://www.forestry.gov.cn/c/www/gtlhbg/147471.jhtml), by 2020, the area under grazing exclusion had reached 0.82 Mkm^2 (Fig. 1e). For the 'no-policy' scenario, the time series of grazed grassland areas was taken from the HYDE3.2, which does not take China's grazing prohibition policy into account (Fig. 1e and Supplementary Table 8).

In ORCHIDEE, vegetation fires can be either simulated prognostically or forced by observations of burned areas. In the model, fires combust surface ground litter and live biomass and result in forest mortality, all of which contribute to CO_2 emissions to the atmosphere. China has a long history of forest fire prevention and suppression stretching from the late Qing Dynasty until after the establishment of the People's Republic of China[56]. However, prevention and suppression have often been ineffective due to poor institutional capacity and low investment. After 1988, this situation changed dramatically, mainly in response to the iconic catastrophic Great Xing'an Mountains fire in May of 1987. Subsequent increases in government budgets for fire prevention and suppression have enhanced the institutional capacities of China's emergency response agencies, leading to a clear reduction in burned areas after 1987 compared to previous years (Fig. 1f and Supplementary Table 8). However, none of the state-of-the-art large-scale fire modules embedded in process-based vegetation models incorporate such dramatic enhancements in fire prevention and suppression in China. The five vegetation models participating in the Fire Model Intercomparison Project (FireMIP) failed to capture the reductions in burned area in China over the past 60 years (supplementary Fig. 17). Hence, to incorporate the carbon cycle effects of forest fire prevention and suppression, the prognostic fire module was not used and, instead, ORCHIDEE was forced with observed forest burned area data. For the 'no-policy' scenario, the simulated burned areas from FireMIP models were used, to represent the case where the dynamics of forest fires were dominated by climate variations rather than by changes in fire management (Supplementary Table 8 and Supplementary Fig. 17).

Simulation setup and attributing the carbon cycle effects

A set of factorial simulations were performed to diagnose the contributions of changes in land management and environmental changes to the terrestrial carbon balance over 1981–2020 in China (for detailed descriptions of all simulations refer to Supplementary Tables 9 and 10). Quantification of the contributions of land management changes made distinctions for the different land use aspects described above, but the effects of reduced timber harvest and reduced rural fuelwood extraction were lumped together. Environmental changes included climate change and atmospheric CO_2 growth. Climate change includes changes in air temperature, precipitation, specific humidity, wind speed, longwave and shortwave radiation, and atmospheric pressure. Although nitrogen deposition has also been reported to contribute to the terrestrial carbon sink in China[57], it was not included in this study because the ORCHIDEE version used here did not include the full nitrogen cycling process.

The terrestrial carbon balance was quantified as NBP, which is NPP minus heterotrophic respiration, fire carbon emissions, immediate carbon emissions following deforestation, extended emissions from

timber product degradation, carbon emissions from rural fuel burning (assumed to be emitted during the year of extraction), agricultural harvest (assumed to be emitted during the year of harvest), and carbon respiration and CH_4 emissions from domestic grazers.

A transient simulation (S_{actual}) covering 1801–2020, in which both environmental changes and changes in land management in the real world were accounted for, was first performed to provide an estimate of NBP over China. The simulated NBP produced by S_{actual} (NBP_{actual}) over 2001–2020 was benchmarked with the estimated terrestrial carbon balance from other approaches (Fig. 2a). Then, starting in 1981, a contrasting simulation $S_{baseline}$ was branched from S_{actual}. In $S_{baseline}$, the climate of 1961–1980 and a constant (1980 value) of the atmospheric CO_2 concentration were used along with the 'no-policy' land management. The $S_{baseline}$ simulation hence provides an estimate of NBP ($NBP_{baseline}$) for 1981–2020 that China would have 'inherited' from the 1960s–1970s conditions, given no changes in environmental conditions or land management but with the legacy effects of all land use activities before 1981. The difference between NBP_{actual} and $NBP_{baseline}$ over 1981–2020 hence yields the collective carbon cycle effects of changes in land management and environmental changes, expressed as Eq. (1):

$$NBP_{actual} = NBP_{baseline} + \sum_{i=1}^{6} C_i \quad (1)$$

where C_i represents the contribution of each environmental or land management change factor to China's terrestrial carbon balance, namely climate change, atmospheric CO_2 concentration growth, afforestation and reforestation, reduced wood extraction, grassland grazing exclusion and forest fire suppression.

The individual contributions of each environmental or land management change factor were further quantified by performing another six factorial simulations (Supplementary Tables 9 and 10), with each being branched from S_{actual} in 1981 but with either no climate change or CO_2 change or with one of the 'no-policy' land management effects. The difference in NBP between each of these six simulations and S_{actual} was used to partition the difference between NBP_{actual} and $NBP_{baseline}$ to derive the contribution of each factor to the terrestrial carbon balance in China:

$$C_i = \frac{NBP_{actual} - NBP_i}{\sum_{i=1}^{6}(NBP_{actual} - NBP_i)} \times (NBP_{actual} - NBP_{baseline}) \quad (2)$$

where NBP_i represents the simulated NBP for different factorial simulations in Supplementary Table 9. Note that in this approach, the quantified contribution of a given factor includes both the direct effect and the interactive effects between the concerned factor and other factors[20]. To further separate the direct versus the interactive effect, additional simulations were performed to quantify the direct effects of individual factors, where actual time-varying values were used for only one of the factors (climate, atmospheric CO_2 or land management) with the values of other factors being the same as in the $S_{baseline}$ simulation (Supplementary Tables 11 and 12).

The simulation design described above was made to cater for our specific research purpose. For this reason, we did not follow the standard simulation protocols of established multi-model simulations such as TRENDY[3] or the Inter-Sectoral Impact Model Intercomparison Project (ISIMIP)[58]. But simulation designs similar to our study, with similar research objectives, have been used in previous studies[15,20].

Forcing datasets for different factorial simulations

In this section, we will first focus on forcing datasets for the S_{actual} simulation and then on factorial simulations with the 'no-policy' land management scenarios. All forcing datasets were gridded at a 0.5° spatial resolution. Below we focus on descriptions of forcing data at the national scale. Detailed information for all the datasets used is given in Supplementary Table 13. We did not directly use the land use forcing datasets of the ISIMIP or TRENDY projects because their land use forcing data were based on HYDE3.2 or LUH2 which do not reflect the actual land management changes in China, in particular for forest area and grassland grazing (Fig. 1). This deficiency in HYDE3.2 or LUH2 has also been described in previous studies focusing on China[15].

(1) Forcing datasets for the S_{actual} simulation. The S_{actual} simulation was preceded by a spinup simulation forced by cycling CRUJRA (Climatic Research Unit and Japanese reanalysis) climate data for 1901–1920, a constant atmospheric CO_2 concentration of 282.54 ppm (the value in 1800), and a static map of the PFT distribution in 1800. The spinup simulation lasted for 380 years, with an additional 20,000 years for a dedicated soil carbon module to speed up soil carbon equilibration until both soil organic carbon and biomass carbon stabilized. The CRUJRA climate data has been widely used by DGVM communities and in particular was adopted by TRENDY simulations made for the global carbon budget assessments carried out by the GCP[3].

For the period of 1801–1900 of the S_{actual} simulation, climate data for 1901–1920 were cycled. Subsequently, time-varying climate data were used until 2020. Annually changing atmospheric CO_2 concentrations were applied for 1801–2020. To incorporate the land use effects of changes in land management, S_{actual} was forced with time-varying PFT maps that accounted for afforestation and reforestation and grazing exclusion, and time series of gridded data for timber harvest and rural fuelwood extraction, and observation-based forest burned areas. All these forcing data cover the period 1801–2020 (Supplementary Method 1).

The time series of annual forest areas for China was produced by combining eight NFIs (the 2nd to the 9th) covering 1977–2018, the national forest area for 2020 reported by the FAO, and dedicated forest area reconstructions for China for several historical years (1700, 1750, 1800, 1850, 1900 and 1949, see He et al. [59]). Linear interpolations were used to fill gaps in the data. Although a greater uncertainty might exist in forest areas before 1977, forest areas reported by China's forest inventory and FAO (also from reports by Chinese government) after 1977 are highly reliable given the massive resources put into the inventory efforts.

The national cropland area for 2015 was obtained from the China Statistical Yearbook. The cropland area in 2015 was used as the base year to adjust the time series of cropland areas for China reported by HYDE3.2, which provided annual cropland area time series for 1800–2015. The national cropland area for 2016–2019 was derived from the China Statistical Yearbook. Because the cropland area for 2020 was not available in the China Statistical Yearbook, it was assumed to be the same as in 2019.

Annual time series of grazed grassland areas were taken from HYDE3.2 for 1800–2015 by summing the 'pasture' and 'rangeland' values. After 2015, national grazed grassland areas were assumed unchanged. However, HYDE3.2 does not account for China's grazing exclusion policy. Hence for the S_{actual} simulation, the area of grazed grassland was adjusted by subtracting the areas under grazing exclusion reported by the National Grassland Monitoring Report, which reports grazing exclusion areas for 2003–2020.

Historical domestic livestock numbers and production at the national level for 1860–2012 were obtained from FAO and Mitchell[60], following conversion to livestock units (LU) based on calculation of the metabolizable energy requirement[61,62]. For the years after 2012, the grazing stocking rates were extended to 2018 using the same approach but with updated statistics from 2013–2018[63], and the values for 2018 were used for 2019 and 2020. The grazing stocking rate during 1800–1859 was assumed to be constant at the 1860 value.

Finally, natural grassland areas were derived as the residual by subtracting the total areas of forest, cropland, grazed grassland, and bare soil from the total national land area. The maximum area for bare land (excluding built-up areas) and urban areas were first taken from China's Land-Use/Cover Dataset (CLUD-A) and HYDE3.2 and then summed together and used to represent 'bare soil', whose spatial distribution was assumed constant over time.

The annual national timber harvest volumes for 1961–2020 were obtained from FAO. Timber harvest prior to 1961 was obtained by multiplying the per capita production in 1961 by the national population reconstructions[64]. Wood volume was converted to carbon using a wood density of 0.6 Mg m^{-3} and a carbon concentration of 50% following Houghton et al. [65].

Tao et al. [17] reported rural fuelwood consumption for China (including charcoal, fuelwood and brushwood) based on a systematic ground survey of 34,489 households distributed across 346 prefectures. Their study demonstrated that government statistics of rural fuelwood consumption were unreliable. Hence, we used their data for annual rural fuelwood extraction for 1992–2012. Fuelwood extraction for 2013–2020 was obtained by extrapolation based on a linear regression of rural fuel consumption with time for each of the 346 prefectures covering almost all of China (see Supplementary Fig. 18 for R^2 distribution of the regressions used for extrapolation). Fuelwood extraction before 1992 was estimated using the per capita fuelwood consumption in 1992 and the annual rural populations for 1800–1991 based on HYDE3.2.

Annual forest burned areas for 1950–2020 were obtained from China's official statistics, which showed good agreement with satellite-based observations for 1995–2016 (Supplementary Fig. 17). Burned areas for 1800–1949 were based on the mean value of simulated burned areas from the five FireMIP models, after correction for the period of 1950–1980 using government statistics (Supplementary Fig. 17). During 1950–1980, burned area dynamics were believed to be driven by climate variations rather than by active fire prevention and suppression, justifying the correction of FireMIP burned area data during this period.

(2) Forcing datasets for factorial simulations of the 'no-policy' land management scenarios. National forest area under the 'no-policy' scenario was assumed unchanged from 1980. Timber harvest for 1981–2020 for the 'no-policy' scenario was obtained by adding the net-imported timber on top of domestic production. The volumes of net import for industrial round wood (including both coniferous and non-coniferous) were obtained from FAO for 1990–2020, followed by further conversion to carbon. Rural fuelwood extraction for the 'no-policy' scenario was obtained by multiplying per capita fuelwood demand in 1992 by the rural populations for 1993–2020, assuming no changes in the rural energy use mix after 1992. Grazed grassland area given in the HYDE3.2 database was taken as the 'no-policy' scenario because it does not account for China's grazing exclusion policy. For forest fires under the 'no-policy' scenario, i.e. without active fire prevention and suppression, the mean values of simulated burn areas for 1981–2012 from the five FireMIP models were used, after correction for the overlapping period with government statistics (1950–1980). Burned areas for 2013–2020 were obtained by random sampling from those between 1981 and 2012.

Uncertainties in land use data and spatial allocation

The land use forcing data after 1980 for the S_{actual} simulation used in this study are statistical data from government or international organizations (e.g. FAO) or ground surveys. No uncertainty information was provided in these original data sources. Hence the uncertainty (standard deviation) for data of each land use type was determined based on expert judgement by accounting for various considerations such as the amount of resources invested in obtaining the statistical data and regulatory strictness.

Forest inventory provides the official and one of the most reliable data sources of forest area in China. Forest inventory is made every five years and is organized in a systematic manner by the National Forestry and Grassland Administration with massive resource investment. For example, the 9th NFI (2014–2018) spent a total of 797 million RMB with 21,300 personnel being mobilized. Forest area data obtained by NFI in China are thus considered to be highly reliable and we assign a 10% relative error in the annual growth rate of forest area since 1980. Timber harvest data were retrieved from FAO which was also sourced from National Forestry and Grassland Administration of China, for which we also assigned a relative error of 10%. The statistics of grazing exclusion area involve a ground survey of local herders but the investigative standards are expected to be less strict than for NFI and we hence assign a relative error of 20%. For fuelwood extraction, annual rural fuelwood extraction was obtained by surveying 34,489 households in China and fuelwood consumptions for historical years (including 1992, 2002, and 2007) were obtained by recall[17]. We thus assumed a 20% relative error in fuelwood extraction. Since China implements strict regulations on preventing and suppressing forest fires, the reporting of burned area by forest fires are is considered highly reliable. We hence assigned a relative error of 20% in statistical forest fire burned area data.

To account for uncertainties in the land use forcings described above, all the simulations in Supplementary Table 9, except for $S_{baseline}$, were repeated three times, to represent the best estimate and the upper and lower estimates of contributions of land management changes to the terrestrial ecosystem carbon balance. Uncertainties in land management for the 'no-policy' scenarios were omitted because they could be implicitly accounted for as the difference between actual land management and the 'no-policy' scenario. The measurement of atmospheric CO_2 concentration is highly reliable and its uncertainty was omitted. The uncertainty in climate forcing data was also omitted because explicitly accounting for it by using another climate data set would have duplicated all simulations and increased computing expenditure. In any case, the CRUJRA climate data has been widely used in DGVM simulations and the uncertainty in the contributions of climate change could be implicitly derived by taking the complement of the contributions from land management. In addition, we did not perform simulations using multiple models because there are currently no other models that include all of the land management processes considered in this study.

Information on the spatial disaggregation of land use and land management data from national to grid cell scales is provided in detail in Supplementary Method 1 and summarized in Supplementary Table 6. The spatial allocation of prefectural, provincial or national total values of land use and land management to grid cells either follows satellite observations and state-of-the-art land use products or, when no such observation-based datasets are available, is based on reasonable assumptions. Often, there are no alternative more reliable datasets which allow quantitative investigation of spatial allocation errors and uncertainties (with the exception of cropland areas, see Supplementary Discussion 1). Hence, we deem it adequate to provide a qualitative assessment of the uncertainty (Supplementary Table 6) in the spatial pattern of land use and land management.

Model parameterization and evaluation

To ensure the model's capability to simulate forest growth and vegetation productivity for China, the model parameters for photosynthetic capacity, autotrophic respiration and biomass residence time were manually tuned (for parameter values see Supplementary Table 7), guided by objective model validation. We first collected a data set from the literature that included forest type, stand age, location, and aboveground biomass carbon stock. Given that the observed forest biomass carbon stocks for different ages (up to 150 years) were under the historical influence of constantly changing CO_2

concentrations, both pre-industrial (282.54 ppm) and contemporary CO_2 (412.10 ppm) concentrations were used to force the model for biomass growth validation. As is shown in Supplementary Fig. 4, the simulated aboveground biomass carbon stock as a function of forest age agreed well with the observations for six different forest PFTs. This suggests that ORCHIDEE can capture biomass carbon growth associated with secondary forest recovery well. Modelled annual GPP and NPP for China under the S_{actual} simulation were compared for 1981–2020 with various estimates based on site-measurement upscaling, remote sensing, and model simulations. As is shown in Supplementary Fig. 15, both our simulated GPP and NPP fell within the range of these other estimates and exhibited a remarkable upward trend over the past decades which was also shared by the other estimates.

The agreements of simulated GPP and NPP with other estimates justify the tuned parameters of photosynthesis capacity and autotrophic respiration. The dual constraining of modelled NPP and forest biomass growth further justifies the validity of the tuned biomass residence time. The sensitivity of NPP and biomass carbon stock—key variables that are influenced by parameter tuning—to atmospheric CO_2 concentration modelled in this study, was an increase by 12.7% and 15.8% per 100 ppm increase in atmospheric CO_2 concentration. These values fall within or are close to, the range of atmospheric CO_2 sensitivity obtained by a recent synthesis of CO_2 enrichment experiments (for NPP, the range is [1.4%, 14.2%]; for biomass stock, the range is [8.1%, 15.2%])[32], justifying a credible CO_2 fertilization effect quantified in our study. Compared to observations, the CO_2 sensitivities for NPP and for biomass in our study seem at the higher end, likely because the CO_2 effect partly implicitly accounted for the effect of nitrogen deposition in China because the model is tuned to fit the observations which are under the influence of nitrogen deposition in the real world. The temperature sensitivity of NPP by ORCHIDEE was reviewed in a previous study and showed broad agreement with results from warming manipulation experiments[66]. The terrestrial ecosystem carbon cycle simulated by ORCHIDEE in response to climate variations in China was also compared with other studies and its plausibility discussed in the main text.

Data availability

The HYDE3.2 datasets are available at https://easy.dans.knaw.nl/ui/datasets/id/easy-dataset:74467/tab/2. The MODIS MCD64A1 data were freely obtained from NASA's Earth Observing System Data and Information https://ladsweb.modaps.eosdis.nasa.gov/. The Global Forest Change data are available at: http://earthenginepartners.appspot.com/science-2013-global-forest/download_v1.6.html. Global Fire Emissions Database is available at https://www.geo.vu.nl/~gwerf/GFED/GFED4/. The CRUJRA data and the corresponding diffuse radiation fraction data used in this study are available at https://catalogue.ceda.ac.uk/uuid/7f785c0e80aa4df2b39d068ce7351bbb. The datasets used to generate all the figures in the Article and its Supplementary Information are publicly available at Figshare (https://doi.org/10.6084/m9.figshare.23574273).

Code availability

The scripts used to generate all the figures in the Article and its Supplementary Information are available at Figshare (https://doi.org/10.6084/m9.figshare.23574273).

References

1. Houghton, R. A. Terrestrial fluxes of carbon in GCP carbon budgets. *Glob. Change Biol.* **26**, 3006–3014 (2020).
2. Lu, F. et al. Effects of national ecological restoration projects on carbon sequestration in China from 2001 to 2010. *Proc. Natl Acad. Sci. USA* **115**, 4039–4044 (2018).
3. Friedlingstein, P. et al. Global carbon budget 2021. *Earth Syst. Sci. Data* **14**, 1917–2005 (2022).
4. Grassi, G. et al. Carbon fluxes from land 2000–2020: bringing clarity to countries' reporting. *Earth Syst. Sci. Data* **14**, 4643–4666 (2022).
5. Roe, S. et al. Contribution of the land sector to a 1.5 °C world. *Nat. Clim. Change* **9**, 817–828 (2019).
6. Grassi, G. et al. Reconciling global-model estimates and country reporting of anthropogenic forest CO_2 sinks. *Nat. Clim. Change* **8**, 914–920 (2018).
7. Griscom, B. W. et al. Natural climate solutions. *Proc. Natl Acad. Sci.* **114**, 11645–11650 (2017).
8. Lu, N. et al. Biophysical and economic constraints on China's natural climate solutions. *Nat. Clim. Change* **12**, 847–853 (2022).
9. Fargione, J. E. et al. Natural climate solutions for the United States. *Sci. Adv.* **4**, eaat1869 (2018).
10. Drever, C. R. et al. Natural climate solutions for Canada. *Sci. Adv.* **7**, eabd6034 (2021).
11. Arneth, A. et al. Historical carbon dioxide emissions caused by land-use changes are possibly larger than assumed. *Nat. Geosci.* **10**, 79–84 (2017).
12. Chen, Y. et al. Accelerated increase in vegetation carbon sequestration in China after 2010: a turning point resulting from climate and human interaction. *Glob. Chang Biol.* **27**, 5848–5864 (2021).
13. Yue, C., Ciais, P., Houghton, R. A. & Nassikas, A. A. Contribution of land use to the interannual variability of the land carbon cycle. *Nat. Commun.* **11**, 1–11 (2020).
14. Bryan, B. A. et al. China's response to a national land-system sustainability emergency. *Nature* **559**, 193–204 (2018).
15. Yu, Z. et al. Forest expansion dominates China's land carbon sink since 1980. *Nat. Commun.* **13**, 5374 (2022).
16. Delang, C. O. & Wang, W. Chinese forest policy reforms after 1998: the case of the Natural Forest Protection Program and the Slope Land Conversion Program. *Int. For. Rev.* **15**, 290–304 (2013).
17. Tao, S. et al. Quantifying the rural residential energy transition in China from 1992 to 2012 through a representative national survey. *Nat. Energy* **3**, 567–573 (2018).
18. Piao, S., He, Y., Wang, X. & Chen, F. Estimation of China's terrestrial ecosystem carbon sink: Methods, progress and prospects. *Sci. China Earth Sci.* **65**, 641–651 (2022).
19. Zhang, L. et al. Interannual variability of terrestrial net ecosystem productivity over China: regional contributions and climate attribution. *Environ. Res. Lett.* **14**, 014003 (2019).
20. Tian, H. et al. China's terrestrial carbon balance: contributions from multiple global change factors. *Glob. Biogeochem. Cycles* **25**, GB1007 (2011).
21. Fang, J. et al. Forest biomass carbon sinks in East Asia, with special reference to the relative contributions of forest expansion and forest growth. *Glob. Change Biol.* **20**, 2019–2030 (2014).
22. Fang, J., Yu, G., Liu, L., Hu, S. & Chapin, F. S. Climate change, human impacts, and carbon sequestration in China. *Proc. Natl Acad. Sci.* **115**, 4015–4020 (2018).
23. Ruehr, S. et al. Evidence and attribution of the enhanced land carbon sink. *Nat. Rev. Earth Environ.* **4**, 518–534 (2023).
24. Piao, S. et al. Evidence for a weakening relationship between interannual temperature variability and northern vegetation activity. *Nat. Commun.* **5**, 5018 (2014).
25. Wei, D. et al. Plant uptake of CO_2 outpaces losses from permafrost and plant respiration on the Tibetan Plateau. *Proc. Natl Acad. Sci.* **118**, e2015283118 (2021).
26. Xu, X., et al. Spatio-temporal patterns of the area experiencing negative vegetation growth anomalies in China over the last three decades. *Environ. Res. Lett.* **7**, 035701 (2012).
27. Zhang, L., et al. Drought events and their effects on vegetation productivity in China. *Ecosphere* **7**, e01591 (2016).
28. Li, X. et al. The impact of the 2009/2010 drought on vegetation growth and terrestrial carbon balance in Southwest China. *Agric. For. Meteorol.* **269-270**, 239–248 (2019).

29. Yuan, W. et al. Severe summer heatwave and drought strongly reduced carbon uptake in Southern China. *Sci. Rep.* **6**, 18813 (2016).
30. Yang, Y. et al. Terrestrial carbon sinks in China and around the world and their contribution to carbon neutrality. *Sci. China Life Sci.* **65**, 861–895 (2022).
31. Deng, L. et al. Carbon in Chinese grasslands: meta-analysis and theory of grazing effects. *Carbon Res.* **2**, 19 (2023).
32. Song, J. et al. A meta-analysis of 1,119 manipulative experiments on terrestrial carbon-cycling responses to global change. *Nat. Ecol. Evol.* **3**, 1309–1320 (2019).
33. Yu, G. et al. Stabilization of atmospheric nitrogen deposition in China over the past decade. *Nat. Geosci.* **12**, 424–429 (2019).
34. Liu, L., Wen, Z., Liu, S., Zhang, X. & Liu, X. Decline in atmospheric nitrogen deposition in China between 2010 and 2020. *Nat. Geosci.* **17**, 1–4 (2024).
35. Ma, M., Cao, J., Tong, D., Zheng, B. & Zhao, Y. Spatial and temporal evolution of future atmospheric reactive nitrogen deposition in China under different climate change mitigation strategies. *EGUsphere* **2024**, 1–50 (2024).
36. Gu, B. et al. Cleaning up nitrogen pollution may reduce future carbon sinks. *Glob. Environ. Change* **48**, 56–66 (2018).
37. Tang, X. et al. Carbon pools in China's terrestrial ecosystems: new estimates based on an intensive field survey. *Proc. Natl Acad. Sci. USA* **115**, 4021–4026 (2018).
38. Yue, Y. et al. Lateral transport of soil carbon and land-atmosphere CO_2 flux induced by water erosion in China. *Proc. Natl Acad. Sci.* **113**, 6617–6622 (2016).
39. Pugh, T. A. et al. Role of forest regrowth in global carbon sink dynamics. *Proc. Natl Acad. Sci.* **116**, 4382–4387 (2019).
40. Yang, H. et al. Global increase in biomass carbon stock dominated by growth of northern young forests over past decade. *Nat. Geosci.* **16**, 886–892 (2023).
41. Leng, Y. et al. Forest aging limits future carbon sink in China. *One Earth* **7**, 822–834 (2024).
42. Yu, Z. et al. Maximizing carbon sequestration potential in Chinese forests through optimal management. *Nat. Commun.* **15**, 3154 (2024).
43. Zhang, X. et al. A large but transient carbon sink from urbanization and rural depopulation in China. *Nat. Sustain.* **5**, 321–328 (2022).
44. Tilman, D. et al. Fire suppression and ecosystem carbon storage. *Ecology* **81**, 2680–2685 (2000).
45. Houghton, R. A. & Castanho, A. Annual emissions of carbon from land use, land-use change, and forestry 1850–2020. *Earth Syst. Sci. Data Discuss.* **2022**, 1–36 (2022).
46. Pan, Y. et al. The enduring world forest carbon sink. *Nature* **631**, 563–569 (2024).
47. Piao, S., Yue, C., Ding, J. & Guo, Z. Perspectives on the role of terrestrial ecosystems in the 'carbon neutrality' strategy. *Sci. China Earth Sci.* **65**, 1178–1186 (2022).
48. Xu, H., Yue, C., Zhang, Y., Liu, D. & Piao, S. Forestation at the right time with the right species can generate persistent carbon benefits in China. *Proc. Natl Acad. Sci.* **120**, e2304988120 (2023).
49. Anderegg, W. R. et al. Climate-driven risks to the climate mitigation potential of forests. *Science* **368**, eaaz7005 (2020).
50. Regnier, P., Resplandy, L., Najjar, R. G. & Ciais, P. The land-to-ocean loops of the global carbon cycle. *Nature* **603**, 401–410 (2022).
51. Krinner, G. et al. A dynamic global vegetation model for studies of the coupled atmosphere-biosphere system. *Global Biogeochem. Cycles* **19**, GB1015 (2005).
52. Ciais, P. et al. Europe-wide reduction in primary productivity caused by the heat and drought in 2003. *Nature* **437**, 529–533 (2005).
53. Piao, S. et al. Changes in climate and land use have a larger direct impact than rising CO_2 on global river runoff trends. *Proc. Natl Acad. Sci.* **104**, 15242–15247 (2007).
54. Yue, C. et al. Representing anthropogenic gross land use change, wood harvest, and forest age dynamics in a global vegetation model ORCHIDEE-MICT v8. 4.2. *Geosci. Model Dev.* **11**, 409–428 (2018).
55. Zhao, J. et al. Spatiotemporal patterns of fire-driven forest mortality in China. *For. Ecol. Manag.* **529**, 120678 (2023).
56. Hayes, J. P. Fire suppression and the wildfire paradox in contemporary China: policies, resilience, and effects in Chinese fire regimes. *Hum. Ecol.* **49**, 19–32 (2020).
57. Liu, X. et al. Enhanced nitrogen deposition over China. *Nature* **494**, 459–462 (2013).
58. Warszawski, L. et al. The Inter-Sectoral Impact Model Intercomparison Project (ISI–MIP): project framework. *Proc. Natl Acad. Sci.* **111**, 3228–3232 (2014).
59. He, F., Ge, Q., Dai, J. & Rao, Y. Forest change of China in recent 300 years. *J. Geographical Sci.* **18**, 59–72 (2008).
60. Mitchell, B. *International historical statistics: Europe 1750–1993*. (Springer, 1998).
61. Chang, J. et al. Climate warming from managed grasslands cancels the cooling effect of carbon sinks in sparsely grazed and natural grasslands. *Nat. Commun.* **12**, 118 (2021).
62. Chang, J. et al. The greenhouse gas balance of European grasslands. *Glob. Chang Biol.* **21**, 3748–3761 (2015).
63. Chang, J. et al. Reply to Comment by Rigolot on "Narratives Behind Livestock Methane Mitigation Studies Matter". *AGU Advances* **2**, e2021AV000549 (2021).
64. Durand, J. D. The Population Statistics of China, A.D. 2-1953. *Popul. Stud.* **13**, 209–256 (1960).
65. Houghton, R. A. & Nassikas, A. A. Global and regional fluxes of carbon from land use and land cover change 1850-2015. *Glob. Biogeochem. Cycles* **31**, 456–472 (2017).
66. Piao, S. et al. Evaluation of terrestrial carbon cycle models for their response to climate variability and to CO2 trends. *Glob. change Biol.* **19**, 2117–2132 (2013).

Acknowledgements

This study was supported by the Second Tibetan Plateau Scientific Expedition and Research Program (2022QZKK0101, C.Y.), the National Key Research and Development Program of China (2023YFB3907403, C.Y.), the Strategic Priority Research Program of Chinese Academy of Sciences (XDB40000000, C.Y.), the National Natural Science Foundation of China (72473111, H.Z.; U2243225, L.D.), the China Geological Survey Project (DD20220877, C.X.), the ANR BMBF French German AI4FOREST (ANR-22-FAI1-0002, P.C.), the ANR CLAND Convergence Institute (16-CONV-0003, P.C.), and the Open-end Funds of Ministry of Education Key Laboratory for Earth System Modelling (Tsinghua University, C.Y. and J.C.).

Author contributions

C.Y. and S.P. designed the study. M.X performed the analysis. C.Y. performed the model development. J.Z. provided forest fire mortality data. P.C., S.T. and W.L. contributed to the interpretation of the results and to the writing. H.S. provided rural wood extraction data. C.Y. and M.X. wrote the first draft together. C.X., H.Z., P.Z., L.Zhang, Y.Leng, and J.W. extensively edited the manuscript and provided suggestions to revise the graphs. J.C., L.D., Y.Li, L.Zhu, and J. H. provided essential suggestions to improve the manuscript.

Competing interests

The authors declare no competing interests.

Additional information

Supplementary information The online version contains supplementary material available at https://doi.org/10.1038/s41467-024-54100-9.

Correspondence and requests for materials should be addressed to Chao Yue or Shilong Piao.

Peer review information *Nature Communications* thanks the anonymous, reviewer(s) for their contribution to the peer review of this work. A peer review file is available.